

RF Bandaid: A Fully-Analog and Passive Wireless Interface for Wearable Sensors

VAISHNAVI RANGANATHAN, Microsoft Research, Redmond; Elec. Eng., University Of Washington, Seattle
SIDHANT GUPTA, Microsoft Research, Redmond
JONATHAN LESTER, Microsoft Research, Redmond
JOSHUA R. SMITH, Elec. Eng., University Of Washington, Seattle
DESNEY TAN, Microsoft Research, Redmond

This paper presents a passive wireless RF sensor platform (RFSP), with only analog components, that harvests energy from an RF source and reflects data as a direct subcarrier modulation, thus making it battery free. A fully-analog architecture results in an ultra-low power device (under 200 μW) with a low component count, reducing the physical footprint. We envision such a platform to enable medical sensing systems that fit on a small bandaid like flexible structure, require no-battery, or charging and are able to provide continuous physiological monitoring. To realize this vision, we have developed and optimized a novel RF architecture that 1) directly maps sensor output to frequency modulation and transmits it to a remote receiver processing unit (RPU). This direct frequency mapping allows all further digitization and computation to be moved to the RPU — reducing power and size requirements on the RFSP; 2) harvests energy from the carrier signal transmitted by a simple continuous wave transmitter, thereby requiring no batteries or supercap; and 3) uses backscatter to communicate with the RPU enabling ultra-low power requirements. The total power consumption of our prototype device leveraging this architecture was measured to be between 35 μW and 160 μW . We demonstrate that the RFSP can harvest sufficient power, sense, and communicate continuously without necessity for energy storage at a distance of 4 m from a transmitter emitting a 915 MHz continuous wave at 26 dBm (0.39 W). Prior backscatter systems typically have power budgets of 1 mW and require energy storage (battery or supercap), RFSP's sub 200 μW power consumption provides a significant improvement and longer range for a given TX power. To demonstrate applicability to real-world health sensing and the flexibility to adapt to different sensors, this paper presents results from breathing, heart rate, temperature, and sound sensing applications.

CCS Concepts: • Hardware → Wireless devices;

Additional Key Words and Phrases: Passive devices, energy harvesting, analog sensing, RFID, body-worn sensors, SDR

ACM Reference Format:

Vaishnavi Ranganathan, Sidhant Gupta, Jonathan Lester, Joshua R. Smith, and Desney Tan. 2017. RF Bandaid: A Fully-Analog and Passive Wireless Interface for Wearable Sensors. *Proc. ACM Interact. Mob. Wearable Ubiquitous Technol.* 0, 0, Article 0 (2017), 21 pages. <https://doi.org/00000n.00000n>

1 INTRODUCTION

The first ever passive radio frequency (RF) sensor was the "Great Seal Bug" listening device invented by Leon Theremin in 1945. The Great Seal Bug demonstrated wireless sensing with a passive cavity resonator connected to an antenna for transmitting sound [4]. The Great Seal Bug inspired the creation of modern RFID systems

Authors' addresses: Vaishnavi Ranganathan, Microsoft Research, Redmond; Elec. Eng., University Of Washington, Seattle, Seattle, WA, vnattar@uw.edu; Sidhant Gupta, Microsoft Research, Redmond, Redmond, WA, sidhant@microsoft.com; Jonathan Lester, Microsoft Research, Redmond, Redmond, WA, jonathan.lester@microsoft.com; Joshua R. Smith, Elec. Eng., University Of Washington, Seattle, Seattle, WA, jrs@cs.washington.edu; Desney Tan, Microsoft Research, Redmond, Redmond, WA, desney@microsoft.com.

ACM acknowledges that this contribution was authored or co-authored by an employee, contractor, or affiliate of the United States government. As such, the United States government retains a nonexclusive, royalty-free right to publish or reproduce this article, or to allow others to do so, for government purposes only.

© 2017 Association for Computing Machinery.

2474-9567/2017/0-ART0 \$15.00

<https://doi.org/00000n.00000n>

that come with microprocessors which enable digital communication and on-board computation [16] [17] [14]. Digitization and transmission of digital data provides reliable sensing with better noise tolerance than the simple transmission of amplitude modulation employed by the Great Seal Bug. These digital platforms are great for applications where a smart sensing device is necessary to sense, compute, and perform certain tasks. However, these advantages come with a power budget, device area, and cost tradeoff – in addition to the need to configure the device for specific applications and sensors.

Using 1940s technology, Theremin was able to achieve a wireless, fully battery free, passive, and difficult to detect audio sensor. Motivated by these appealing properties, we looked at the current state of the art in battery free wireless sensors; we found that most approaches focused on utilizing digital logic on the remote sensing portion of their system and/or attempted to build on standards compliant protocols such as RFID. While digital communication has advantages and standards compliance enables the use of off-the-shelf equipment, we realized that there was an opportunity to learn from Theremin’s device and use some of his techniques to build a system with a different set of trade-offs/advantages. Our work is motivated by the need for a wearable, compact, flexible, and potentially one-time use (disposable) sensing platform which could be used in physiological sensing applications such as home monitoring. This work uses three take-aways from Theremin’s Great Seal Bug:

- (1) Added complexity on the infrastructure/receiver is acceptable if it imparts positive attributes to the wearable sensor
- (2) Standards compliance is not critical with the increased availability and commoditization of Software Defined Radios (SDRs)
- (3) Digital components are not a requirement for a wearable sensor (they impart advantages but are not necessary); analog signaling is appropriate and advantageous if you are willing to accept some trade-offs

These three ideas allow us to envision a much simpler wearable sensor. Our work is less concerned with widespread adoption and more with enabling new use-cases, rapid prototyping, and exploring use-cases where the trade-offs of a simpler wearable sensor design are advantageous enough (i.e. enabling a reduced physical size/reduced power consumption) to offset the limitations. Limitations are discussed in Section 5, system designers will need to weigh the advantages of a simpler analog system with the disadvantages and decide whether an RFSP-like system is appropriate for their application.

While RFID based platforms still serve a number of use cases, we found that there was significant scope for improvement in terms of size, components count (essential to make it ‘disposable’), and power requirements by exploring more analog solutions that offload computation to an AC powered receiver. Analog operations are appealing because they reduce the required operating power on the wearable sensor. Lower operating power correlates to increased range without any additional energy storage. Our device has roughly 3-5x the range of similar digital backscatter devices with the same transmit power level [16] due to its lower operating power requirements. In this paper, we present a complementary fully-analog RF Sensing Platform (RFSP) which can interface to a variety of sensors and which maps sensed data into direct frequency modulation, that are backscattered to the Receiver Processing Unit (RPU). This approach has two main goals:

- (1) Moves digitization and computation overhead from the sensing device (RFSP) to the remote RPU - which saves complexity, cost, area, and power on the sensing device.
- (2) Using frequency modulation to encode and transmit data makes it more tolerant to noise and attenuation in comparison to transmitting the data using direct amplitude modulations.

We believe that the analog sensing and backscatter approaches presented here, although not novel (in light of use by surveillance agents for many years and designs being closed-source) have not received appropriate attention by the sensing and IoT community. Backscattering analog signals with frequency modulation is a complementary approach to traditional digital backscattering approaches. We believe this method allows us to create a flexible platform which can be interfaced to a number of analog sensors (resistive or capacitive). The

RFSP presented in this work is currently designed as a development platform. By presenting a detailed account of the RF architecture, component choices, trade-offs, and presenting evidence of its superior functionality we are confident that we can enable follow-up work that benefits from flexible, ultra-low power, small, and battery-free ubiquitous sensing.

Applications that require continuous monitoring (like wearable measurement of physiological signals, temperature monitoring in food/pharmaceutical industry, etc.) benefit from small, flexible low-power devices. Specifically, for applications such as continuous bedside monitoring of physiological signals we need a device that is not only small but comfortable to wear. Our device is configured for a power budget under $200 \mu\text{W}$ for sensing and data transmission. This enables it to be powered by the energy harvested from the incident UHF signal. The bedside monitoring scenario in this case would require a dumb omni-directional transmitter that transmits the UHF continuous wave (CW) signal. The device worn by the patient (envisioned as a disposable fabric band-aid with a tiny circuit board) harvests energy from this signal to perform the sensing and backscatters the sensed data as subcarrier modulation on the UHF signal. This modulation is picked up by a sensitive receiver (the RPU) which could be incorporated into a bedside device (i.e. a bedside clock). The RPU servers as the hub for digitization and processing of data to display the sensed data to care-providers. The TX and the RPU are a one-time installation, while the wearable device is a flexible, low cost (potentially one-time use) bandaïd-like device and which uses the same analog system for different sensing applications. A block representation of this RFSP is provided in Fig. 2.

To understand the RFSP better, Section 2 provides a detailed description of the system design and theory of operation. An analysis of different sensing scenarios and design choices is provided in Section 3. This is followed by results from sensing measurements using the RFSP and an analysis of power consumption and range of the device in Section 4. Finally, a discussion on limitations, related work and methods to address challenges, potential applications and future design improvements is covered in Section 5 and Section 6 provides conclusions to summarize our work.

2 SYSTEM DESIGN AND THEORY OF OPERATION

2.1 RF Sensing Platform Description

There are four main design and operational constraints that we optimize our prototype of RFSP for. First, it should map the sensed signal directly to a frequency modulation. This is what primarily makes it an analog sensing platform. Second, use this modulated frequency to drive an antenna to produce the backscatter effect. In particular, this involves use of an RF switch that is toggled at the desired frequency to produce a subcarrier modulation that rides on the incident UHF signal. Third, to power the sensing, frequency generation and RF switching, energy is needed. This is accomplished by harvesting energy from the incident UHF signal. Finally, to ensure a large practical operational range, the overall power budget needs to be kept low.

Before we discuss system specific component choice and optimizations, we briefly describe the operational principle behind a backscatter device. Consider the Great Seal Bug. It was a mechanical cavity resonator with an antenna such that when energized by illuminating it with a continuous wave RF signal, the specially designed cavity's capacitance and the antenna would form a tuned RF frontend. Any changes in the cavity (and hence its capacitance) caused a 'detuning' of this resonance structure. When sound waves fall on the cavity and create a vibration, these vibration are encoded as a series of capacitance changes and hence a time-varying detuning of the antenna that results in reflecting a slightly varied signal than the original illuminating RF signal. In effect, any sound expressed on the cavity resonator was directly mixed into the illuminating signal and reflected back as an amplitude modulated (AM) signal. Here, the Great Seal Bug resonator acts as a mirror that reflects (hence, the term backscatter) the illuminating source at different frequencies instead of generating its own source for response. This electronics-free operation allowed it to function with only a mechanical cavity and remain undetected for seven years[4]. Backscatter principles have now been adapted as a communication method for several RFID based

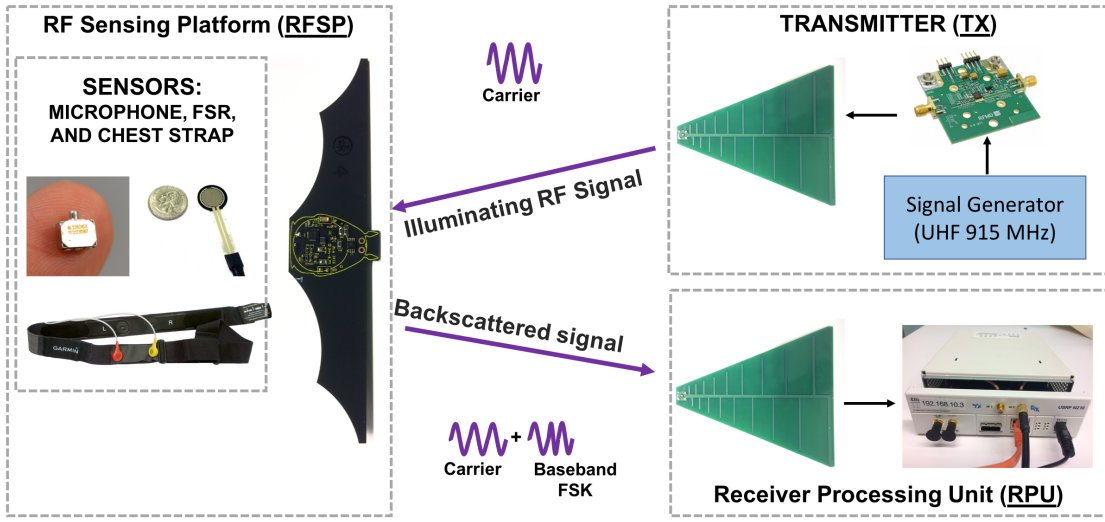


Fig. 1. A system description of the RF Bandaid system with the transmitter and the receiver processing unit (RPU) on the right side and the RF sensing platform (RFSP) with its sensors on the left. The receiver side (the RPU) consists of a Ettus Research N210 Software Defined Radio (with SBX daughterboard) which acquires the backscattered signals. All processing of the backscattered signal is performed on a computer that controls the SDR. The transmitter (TX) side consists of a 915 MHz signal source and a RFMD RF6886PCK-410 linear power amplifier. TX side is a dumb device which outputs a continuous wave (CW) at 915 MHz to provide backscatter power and the carrier signal. The RFSP harvests power from the TX side and maps signals sensed by a resistive/capacitive sensor into a modulated frequency output which is backscattered on the carrier signal. This signal is received and processed by the RPU to display sensor data to user.

sensing and computation systems. Compared to active radio communication, where the sensing device generates the UHF carrier for data transmission, this method (employed by backscatter systems such as RFID) has 100x reduction in power consumption (with devices ranging from several 10s of mW to less than 200 μ W) since there is no active generation of the UHF carrier signal [10][14].

In the RFSP, the varying signal and the detuning (or the signal mixing) of the antenna is implemented using a tunable oscillator and an RF switch. The time varying signal we generate is a frequency modulation such that the frequency varies as a function of the sensor input. For instance, for a resistive pressure sensor, as the resistance decreases with pressure, the frequency increases. The key component that enables this function is a low cost micropower precision programmable oscillator (MPPO) from Linear Technology LTC6906 [9]. This device can be configured to convert a varying resistance at sensor output to set its output frequency. It maps a resistance change in range of 100 kOhm to 1 MOhm into frequencies in range 1 MHz to 10 kHz.

To drive the antenna, we toggle an RF switch across the antenna that acts like a mixer to modulate its switching frequency on top of the incident 915 MHz carrier wave. The communication front end on the RFSP uses the ADG902 reflective wide-band switch from Analog Devices[5]. We chose this particular part because it operates with an ultra-low power consumption and low quiescent current (max 1 μ A). As an added advantage, this analog switch also has low insertion loss (-0.8 dB) and high isolation (-40 dB) properties at 915 MHz. For the RF switch to effectively backscatter, the RF frontend needs to be tuned at 915 Mhz. We accomplish this using a L-matching network that consists of a capacitor in parallel from antenna to ground and an inductor in series.

To interface the sensors that modulate the oscillator, we first use a 100 kOhm resistor to set the minimum required resistance (R_{SET}) at the frequency set pin (SET) of the MPPO and add the sensor in series to it. The next step is to calibrate the resistance change of sensor (R_{Sense}) to vary between 1 kOhm and 900 kOhm with a step resolution of at least 500 Ohms. The limit on the resolution depends on resolution of the ADC on the RPU and its sampling rate. Limiting different sensors to specific variation range in R_{SET} lets us allocate separate channels to different types of RFSP that might be associated with a single RPU. The SET pin on the MPPO is at 650 mV and acts as a current sink to an operational amplifier that sets the master output frequency of a internal voltage controlled oscillator (VCO). This frequency is then divided based on the configured ratio. This pin also has a precision internal capacitance of 10 pF that combines with $R_{SET}(100\text{ kOhm} + R_{Sense})$ to set the oscillation frequency. The output of this MPPO drives the gate of the RF switch for backscattering.

The MPPO IC can operate at a DC voltage range of 2.25 V to 5.5 V, while the RF switch can operate between 1.7 V to 2.75 V. To provide a supply for these two components a Texas Instruments BQ25570 Nano-power buck-boost IC is used to harvest and buffers the small amount of energy for operation in through a small ceramic capacitor ($\sim 50 \mu\text{F}$) [6]. The DC-DC conversion module also has a low dropout regulator which is set by divide resistors to regulate a 2.3 V supply to power the components on the system. BQ25570 was chosen for its ultra-low cold start voltage (330 mV) and high efficiency (greater than 85%) for the power levels being harvested in this application. The IC also provides the means to charge a small battery if this feature becomes necessary for future application-specific instantiations of the RFSP. This design flow is summarized in the block diagram provided in Fig. 2. The specific components for RFSP design were carefully selected to maximize sensing ability while minimizing the cost, area and power consumption. This also helps eliminate the need for a large storage device which makes it possible to develop small, flexible and low cost devices.

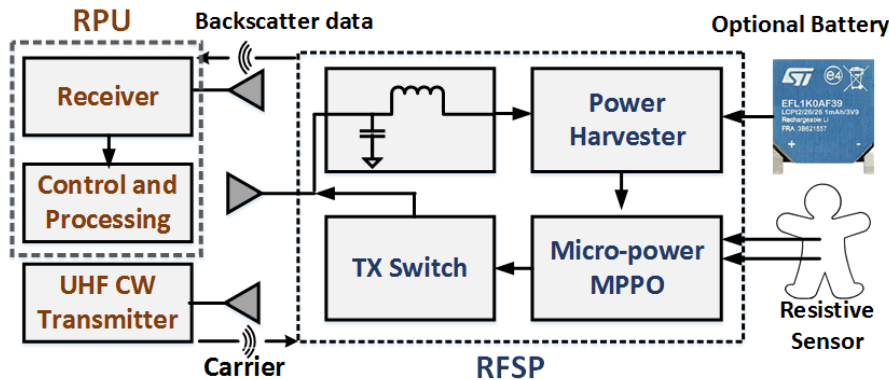


Fig. 2. A block representation of the RF Bandaid system. The RPU and transmitter are shown on the left (RX & TX) and a detailed block diagram of the RFSP is shown on the right. Power from TX is harvested by the RFSP through its front end and power harvester. The power harvester will store charge in a small ceramic capacitor until the capacitor voltage exceeds its set threshold. Once this threshold is reached (currently set to 2.6 V with a hysteresis at 2.4 V—that is, charging doesn't resume until capacitor voltage is below 2.4 V), the power harvester enables a low power LDO or supplies power directly into a resistive sensor (depending on the system designers needs). As the resistive sensor changes, it modulates the output of a low power VCO (MPPO) which controls the gate of a TX switch. This modulation encodes the changes in resistance into a "carrier + sensed FSK" radio signal which is picked up by our receiver path (an SDR in our current system).

2.2 MPPO Configuration

The LTC6906 is a micropower resistor set oscillator which allows its output, f_{out} , to vary between 10 kHz and 1 MHz depending upon the resistance at R_{SET} . Its output, f_{out} , is generated by an internal 1 MHz master oscillator which is followed by a frequency divider which operates according to the following formula:

$$f_{out} = \frac{1\text{MHz}}{N} * \frac{100\text{kOhm}}{R_{SET}} \quad (1)$$

The R_{SET} value determines the master oscillator frequency while the DIV pin sets a division ratio N . For the LTC6906, R_{SET} must be 100 kOhm at a minimum and 1 MOhm at the maximum. The operating range of f_{out} output can be configured for a specific band in this 10 kHz to 1 MHz frequency range by setting a resistor-set clock divider, N . With the master clock of the MPPO fixed at 1 MHz, f_{out} output is calibrated for operation within:

- 100 kHz to 1 MHz by using a clock divider ratio set to 1 [$N = 1$]
- 33.3 kHz to 333.3 kHz by using a clock divider ratio set to 3 [$N = 3$]
- 10 kHz to 100 kHz by using a clock divider ratio set to 10 [$N = 10$]

For any given frequency the power can be minimized by reducing the master oscillator frequency (maximize R_{SET}) and using the lowest possible clock divider ratio ($N = 1$). Specifically, if R_{SET} is at the minimum 100 kOhm, the master oscillator output is at 1 MHz (output is at 100 kHz for the maximum 1MOhm). By setting the clock divider ratio to 10 ($N = 10$), this 1 MHz signal is divided, by 10, to 100 kHz and provided as MPPO output. This setting accounts for a maximum current draw and the RFSP has been characterized for this maximum current draw setting. The measured minimum power consumption of the RFSP is 35 μW when $R_{SET} = 1\text{ MOhm}$ and a divide ratio of $N = 10$ are used. The maximum RFSP power consumption was tested to 160 μW when the R_{SET} was fixed set to 100 KOhm with $N = 10$.

- To interface sensors with resistive variation in 100's of kOhms to MOhms, the actual sensor interface has a 1 MOhm base resistor ($R_{Baseline} = 1\text{ MOhm}$) across the SET pin and R_{Sense} is added in parallel to it (this sets the minimum frequency to 10 kHz without any sensor). As R_{Sense} varies, the R_{SET} value decreases. Thus increasing the R_{Sense} value results in an increase in the MPPO output frequency, up to 1 MHz.
- For sensors with resistance values in the in 10's of kOhms, we use a $R_{Baseline} = 100\text{ kOhm}$ to set the minimum required resistance on the MPPO SET pin. The R_{Sense} value is added in series to this baseline resistor, $R_{Baseline}$. $R_{Sense} = 0$ corresponds to an MPPO output frequency of 1MHz. In this case, increasing values of R_{Sense} correspond with a decrease in the MPPO output frequency, down to 10 kHz.

The current consumption of the MPPO can be calculated using the following equation.

$$I^+ = 5\text{ }\mu\text{A} + (6 * \frac{V_{SET}}{R_{SET}}) + V^+ * f_{out} * (C_{load} + 5\text{ pF}) + \frac{V^+}{2 * R_{load}} \quad (2)$$

Specifically, for the RFSP $V_{SET} = 0.650\text{ V}$ and C_{load} is 2 pF at 1MHz from the ADG902 switch input specifications. With an operation voltage of $V^+ = 2.3\text{ V}$, the value for I_{MAX}^+ is around 61.25 μA (140.87 μW) and I_{MIN}^+ is around 11.6 μA (26.68 μW). These computed values correlate with the overall power consumption that was measured on the RFSP with a minimum of 35 μW and a maximum of 160 μW . As evident, the MPPO is the largest power consuming component in the RFSP.

2.3 Receiver Processing Unit

Since the sensor is designed to harvest energy and communicate data using a 915 MHz front-end, the setup requires a 915 MHz continuous wave transmitter (TX). This can be a standard signal generator or a programmable transmitter module connected to a 915 MHz antenna and can provide sufficient power. The receiver (RX) must be

capable of picking up the backscattered signal and also perform the necessary computation as a back-end. Since this is the smarts of the setup, we implemented it using a USRP N210 software defined radio (SDR) module from Ettus Research [7]. This setup uses a SBX daughterboard (400 MHz to 4400 MHz band) where the RX2 port was configured to receive the backscattered signal. A GNU radio user interface controls the USRP for receiving and processing the data. A python script was used to process the received data and obtain sensed measurement results. The USRP module is capable of more than 40 MHz sampling speed at its ADC, which sets the resolution limit for the sensed signal. We have tested the USRP with 10 MHz sampling rate while processing data in real-time. For our test applications which primarily involve lower frequency signals, we used a 1 MHz sampling rate which supported real time processing and data viewing with GNU radio running on a Lenovo Thinkpad T530.

With our 1 MHz sampling rate we can resolve R_{SET} step variations that are 500 Ohms. For applications which require a higher resolution of R_{SET} (steps variation that are smaller than 500 Ohms). Smaller R_{SET} step variations translate to smaller variations in MPPO output frequency. System designs can perform two optimization, to improve the system. Firstly, improving the sensitivity of the RPU and second, using higher sampling rates at the receiver ADC for better temporal resolution. A higher sampling rate at the receiver unit (for example, the USRP's maximum 40 MHz) allows for a higher temporal resolution of the received signal (versus the 1 MHz sampling rate currently used), allowing the system to track smaller variations in MPPO output frequency. Higher temporal resolution also allows for finer time resolution.

3 APPLICATION-SPECIFIC DESIGN OPTIONS

Range is typically one of the most important parameters for backscatter systems. We have tested the range of the RF Bandaid system with the transmitter (TX) output power set at 26 dBm (390 mW) to be around 4 meters with no duty cycling (that is, the backscatter tag has surplus power and continuously operates) and 2.7 meters with the TX output power at 23 dBm (200 mW), again with no duty cycling. Beyond these ranges the sensor begins to consume more power than it receives and has to duty cycle: turning off to store enough charge before continuing operation. Increasing the range further causes the sensor to drop out completely. Duty cycling of the RFSP allows the sensor to continue to provide useful output. During duty cycling, the RFSP waits until it has enough power to start then begins to perform frequency modulation until it no longer has enough power to operate. The RPU sees this as a reflected signal appearing and then disappearing when the RFSP duty cycles off. In our range tests we used commercial log-periodic 915 MHz antennas for TX and RX, and output power was limited to a max of 26 dBm due to an equipment limitation, the FCC limit of 1W (30 dBm) would enable a bit more range between TX and the sensor. The RFSP tag has a half-wavelength dipole antenna shown in Figure 1 along the wing edge of the bat shaped board. The receiver side antenna (RPU) was placed approximately 10 meters away from the TX antenna and both were not moved during testing, instead the sensor was moved further away from the TX side to test the range.

3.1 RX Placement and RX/TX Antenna Configuration

One interesting property of decoupling RX and TX is that the RFSP is more sensitive to the distance between the sensor and the TX power source (the sensor needs enough TX power to operate). The RX side has more than enough sensitivity so the limiting distance in our system becomes how close the TX power source is to the RFSP. If we place the RFSP close enough to the TX power source so that it has enough operating power we can move the RX antenna much further away (in our tests at least 9+ meters) into another room and still receive data. Because our system only needs a CW transmitter, the TX power sources are much cheaper and simpler (a 915 MHz RF signal source + optional amplifier + antenna) allowing us to distribute TX antennas around while having only a single or a few more complex and expensive RPUs. This allows in a standard home setup to centrally place a high-gain RPU and to distribute dumb TX units around the entire home to power RFSPs throughout the home.

3.2 Operational Range

As with a typical TX-RX setup, the transmitted UHF signal attenuates with distance, governed by Friis path loss equation. Hence, the closer the device is to the TX, the stronger its backscattered signal and the more power that is available for continuous operation. In the applications described so far, a small capacitor is sufficient to smooth out fluctuations in power availability when the TX side is relatively close-by. When the device is further away from TX, it does not receive sufficient power to perform the sensing task. Also, the signal is backscattered on a much smaller amplitude carrier. As the device moves away, it starts duty cycling between being on and off based on power availability. There are four different ways of improving the operational range of this device;

- Move device closer to TX: In some applications, if range permits, having the device close (within 0.5 meters) to the TX allows for more power availability and the RX can be moved further away.
- Increase TX power: We tested the device for range using the 915 MHz log-periodic antenna at TX and a whip antenna at the RPU placed 10 meters apart and moved the device away from the receiver until it started duty-cycling. This distance was recorded to be 3 meters for 23 dBm, 3.6 meters for 24 dBm, 3.8 meters for 25 dBm and 4 meters for 26 dBm. With this diminishing return due to path loss, increasing transmit power if not an ideal resolution.
- Using a battery: To extend the range further we tested the device in the same setting with battery power (a 160 μm thick ultra-thin battery), and 26 dBm at the TX. We observed continuous operation on the device up to 8.8 meters away from the TX.
- Better antennas: We have used simple commercially available antennas for our generic tests. Using application-specific high-gain antennas would enable sensing at further distances as well as better transmission of power and harvesting.

Even though one of the strengths of our system is that it does not require a super capacitor or battery for an energy storage device, it is capable of operating with a battery. For system designers or applications where a battery is acceptable or where the added functionality is worthwhile, batteries are an interesting operating mode. Because the RFSP consumes very little power, a system designer can always choose to add in a small primary cell or rechargeable battery to increase the operating range or reliability of the system. This can be useful for two reasons 1) situations where backscatter power cannot supply enough power for a power hungry sensor and the battery source is used to keep such a sensor running 2) to bridge any gaps in TX coverage to allow for continuous operation. The 2nd option is useful for our proposed monitoring application because our low power draw means we can make use of ultra-thin film rechargeable batteries (such as the ST Microelectronics EFL1K0AF39 [8] which has a paper thin 160 μm total thickness, rated for 1 mAh at 3.9 V). Because we only draw power from the battery when TX received power drops below our power consumption, we normally would consume very little battery current. It should be noted that such thin and low-density batteries have otherwise limited application scenarios. However, coupled with the low current draw of the analog RFSP, batteries open up application scenarios that would otherwise not be practical. When the RFSP has excess TX power it can always charge the battery, helping to make the system far more reliable if needed. Or for more difficult environments or times of severe body occlusions the battery can provide enough power to allow our system to operate continuously for several hours where it would otherwise need to duty cycle.

4 TESTING AND RESULTS

All tests for the RF Bandaid system were performed in the corridors and rooms of a busy office building with no control over the RF environment (Fig. 5c). Many common sensors typically involve a change in resistance or capacitance. One of the strengths of this system is that we can easily interface to a wide variety of resistive or capacitive based sensors. The focus of this work is to measure resistive changes that are mapped into frequency modulation for transmission. Capacitive sensors can be used with impedance transformation with circuits such

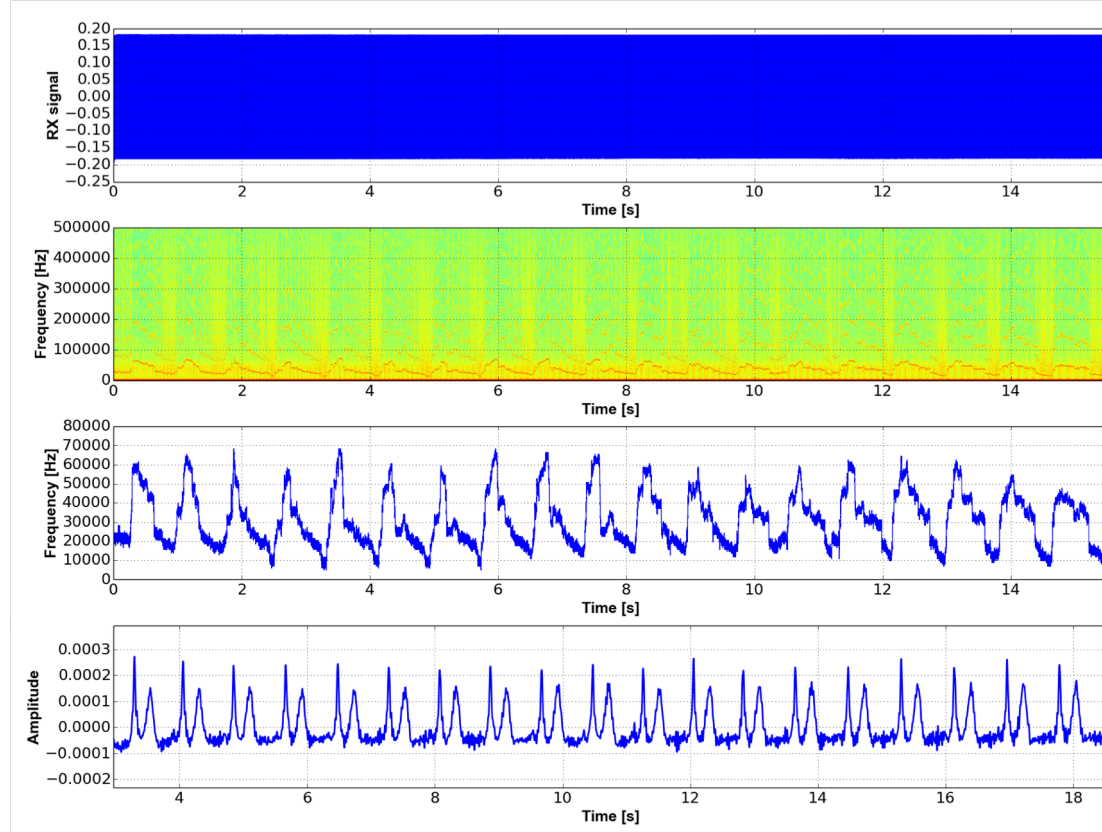


Fig. 3. Received and processed signals for heart rate sensing. The plots show the raw time-domain signal, spectrogram, the extracted frequency modulation envelop and EKG measured using a medical grade sensor from top to bottom, respectively. The time-domain signal looks like an envelop function due to the dense signal. The spectrogram shows the encoded signals along with the harmonics, this figure is centered at 915 MHz (0 Hz in this subplot is 915 MHz) and shows harmonics visible within 500 kHz of 915 MHz. And finally the bottom two signals are a raw signal extracted from the spectrogram showing the sensor data and the bottom figure is the EKG ground truth measurement. Both show the 19 pulses measured over 15 seconds of measurement.

as a common-source amplifier. To demonstrate this we examine three different resistive sensors that measure temperature, force, and stress in this section. To demonstrate the use of capacitive sensors with the RFSP we have also tested the system for transmission of audio signals sensed with an electret microphone. These microphones are typically a capacitive cavity with a FET common-source amplifier. The first test demonstrates the use of body-worn resistive sensors to measure physiological parameters. For example: the heart rate of a person can be detected as a pulse in the wrist, chest or neck. Similarly a piezo-resistive stretch sensor can be used to measure breathing rate with expansion of the chest cavity. Force sensing resistors (FSR) are also used for detection and rehabilitation of patients with carpal tunnel syndrome and for posture correction. Other applications like force measurement in prosthetic limbs can also be measured using resistive force and stretch sensors. To interface these sensors with the MPPO, we have calibrated them to vary in the range of 30 kOhm to 500 kOhm and have configured the MPPO for maximum power consumption.

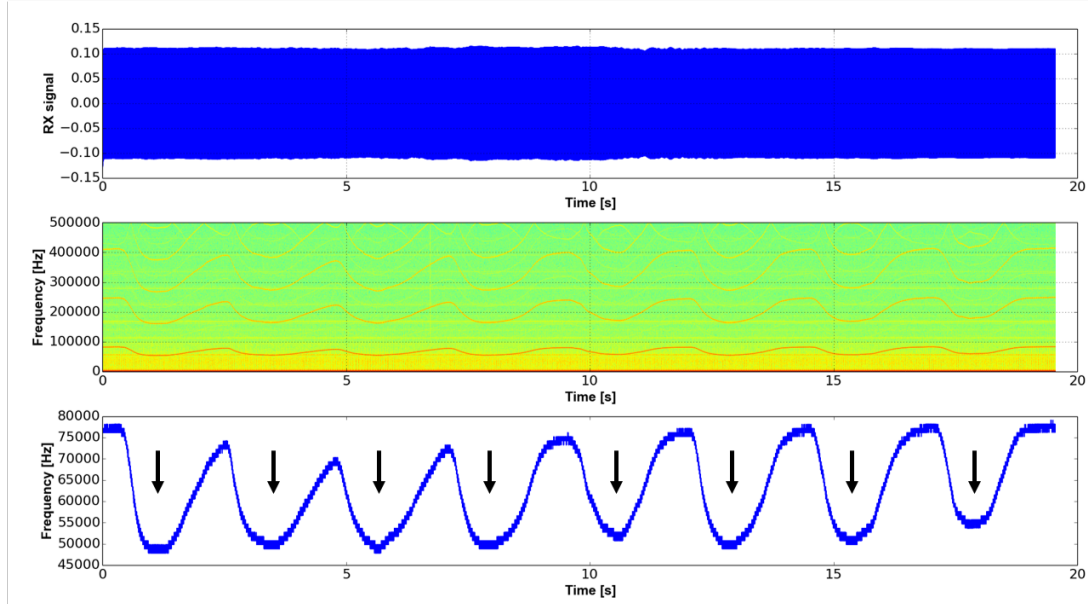


Fig. 4. Received and processed signals for breathing showing the raw time-domain signal, spectrogram and the extracted frequency modulation envelop from top to bottom, respectively. The spectrogram shows the encoded signals along with the harmonics for the breathing sensor, this figure is centered at 915 MHz (0 Hz in this subplot is 915 MHz) and shows harmonics visible within 500 kHz of 915 MHz. And finally the bottom signal is a raw signal extracted from the spectrogram showing the breath sensor data. The arrows indicate the times at which the user starts exhaling. The breathing rate measured here is 8 exhalations in 20 seconds.

The signals received by the SDR are first filtered to the desired band where we expect the frequency modulation. The envelop of the frequency modulation signal is then extracted to obtain the sensed value. Measurements for heart rate, breathing rate, and temperature, using resistive sensors, were tested using the RFSP. Their setup and results are provided in the following sections. The heart rate and breathing rate sensors were tested on four volunteers to verify reliable and reproducible operation.

4.1 Heart Rate Measurement

The RFSP is first tested to measure heart rate in beats per minute. A typical method to detect pulse rate is from the carotid artery in the neck where a distinct pulse can be felt by placing fingers on the neck to the side of the windpipe. The number of pulses felt is counted over 10 seconds to calculate approximate beats per minute. By placing the FSR (R_{sense}) at the neck we can measure the resistive change that corresponds to heart rate.

Three separate trial measurements were taken from four volunteers with our device. To verify this measurement, a parallel study was performed using an industry standard EKG sensor to measure heart rate during the three trials. Fig. 3(a) shows the received signal, a spectrogram obtained from raw received signal, the measured heart rate signal (as frequency modulation) extracted from filtered signal and finally the EKG recording from the ground truth device. On detecting the envelop of the filtered signal we then extracted the pulse rate of around 19 beats in 15 seconds (76 beats per minute). The measurement from our device shows heart beat rates correlating to the measurement from the ground truth device. Since the RPU is capable of high complexity computation, standard signal processing algorithms can be employed for identifying the heart rates from the received signal.

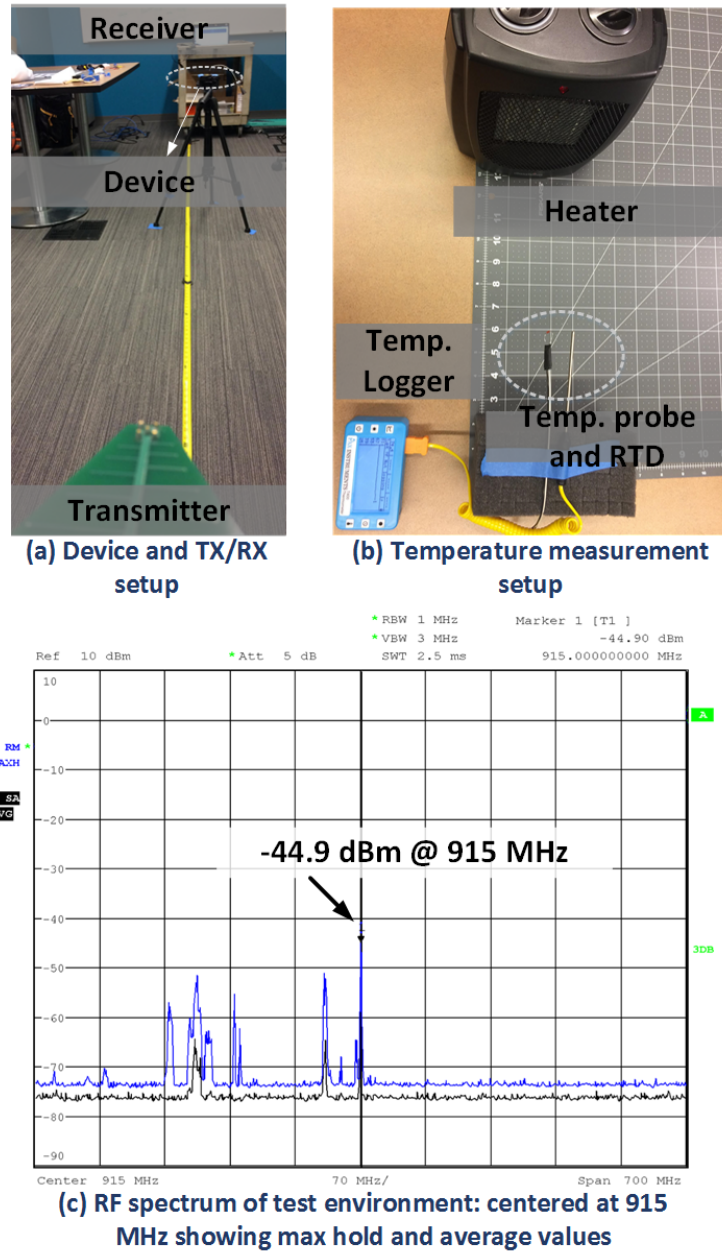


Fig. 5. The experimental setup with TX, the RFSP and the RX is provided in (a). The RFSP is 2.7 meters away from the TX and the RX is placed at 4.3 meters distance from the TX for these experiments. The test setup for ground truth measurement of temperature along with a RTD sensor that interfaces to our prototype is shown in (b). A heater was used to ramp up the temperature after cooling the sensors to 36 °F. (c) Is a spectrum analyzer measurement showing the RF signals present in the test environment

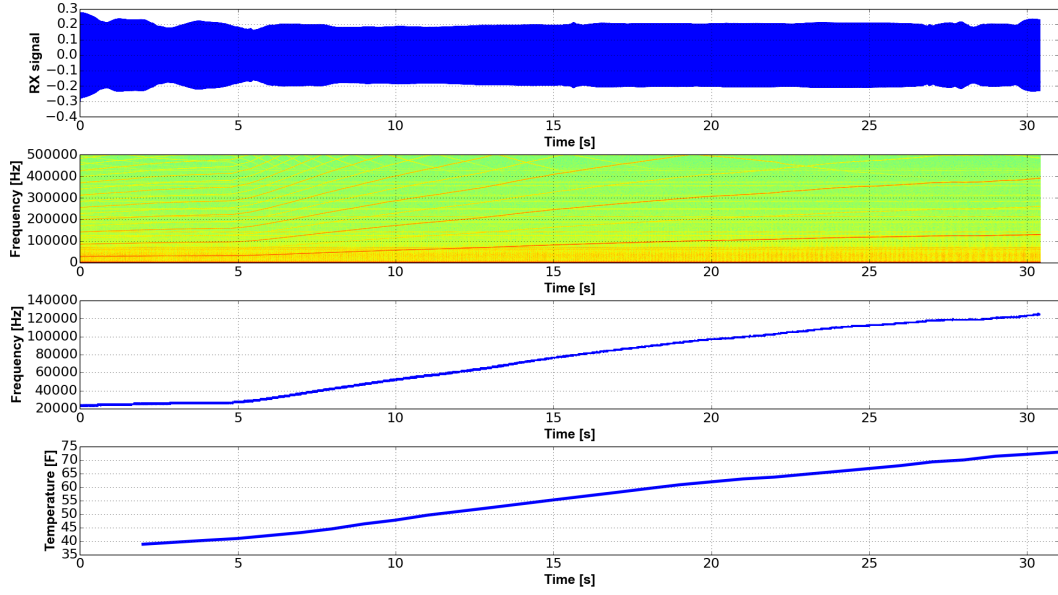


Fig. 6. Received and processed signals for temperature sensor showing the raw time-domain signal, spectrogram, extracted frequency modulation envelop, and ground truth temperature reading from top to bottom, respectively. Similar to 3 we show the time varying RX input signal (which looks like an envelop), spectrogram centered at 915 MHz (0 corresponds to the received 915 MHz carrier), and the extracted temperature signal which corresponds well with the ground truth.

4.2 Breathing Rate Measurement

Several state-of-the-art commercial respiratory monitors use a strap/harness around the chest [1] or in the abdomen [3] for measurement. To leverage this expansion in the chest/abdominal cavity to measure breathing we built a custom strap using a carbon doped fabric that changes resistivity as it stretches [2]. The fabric is sensitive enough to register small elongations or contractions which result in resistive changes on the order of several 10's of kOhms for a few millimeters of stretch. This resistance change is added in parallel to a baseline resistance ($R_{Baseline} = 1$ Mohm) that calibrates the MPPO to its fundamental low frequency output and any R_{Sense} variation increases the output frequency as the overall R_{SET} decreases. Fig.4 shows the raw received signal, the spectrogram of the received signal and the frequency modulation corresponding to breathing extracted from the filtered signal. The test subjects were asked to perform a button push task on exhalation during the test and the timestamps were used to verify the breathing rate. The exhalation points are marked by downward arrows on the extracted signal. A total of 8 breaths were recorded in the 20 seconds of measurement (24 breaths per minute). Similar to heart rate measurement, more complex algorithms can be used to identify the breathing rate since the RPU is not constrained by power limitations.

4.3 Temperature Measurement

To measure non-periodic parameters like pressure and temperature, we use the same technique of transmitting the signals encoded as subcarrier modulation. To demonstrate this we used a standard off-the-shelf resistive temperature detector (RTD) with the RFSP to log temperature changes. We also used a Pax Instruments T400 temperature logger in parallel to log the ground truth data. Both sensors were initially cooled in ice to 36 °F. While logging the temperature, both the sensors were exposed to a space heater that increased the temperature to

Sensor	Part Spec.	Power Range(μW)	Range w/o Battery	Range w/ Battery	Lifetime w/ Battery(Hrs)
Chest Strap (breathing rate)	BodiTrak Smart Fabric	128 to158	<3 m	>4.26 m	~8 to 6.5
FSR (heart rate)	SEN-09375	87 to147	<3 m	>4.26 m	~12.5 to 7
Temperature	254JG1J	87 to 156	<3 m	>4.26 m	~12.5 to 6.5

Table 1. Power consumption, range (TX set to 200 mW or 23dBm), range with an on-board battery source (TX set to 200 mW or 23dBm), and the worst case battery runtime for the breathing, heart rate, and temperature sensors

around 75 °F. The data logged by the RFSP and its respective spectrogram, the extracted frequency modulation and the T400 logger data are provided in Fig.5. The change in frequency corresponding to the change in temperature is observable during the log interval of 30 seconds.

4.4 Audio Transmission With Capacitive Sensor

The sensors incorporated so far are resistive in nature and can be directly used with the MPPO. To interface capacitive sensor we must first convert the sensor variation to a varying current draw from the SET pin. This can be achieved by using common source amplifiers that convert the voltage change with capacitance at the gate of a FET into a current draw change at the drain terminal. To demonstrate this we used an electret microphone (EK23024) by Knowels along with the RFSP. The drain and source of the microphone was connected in parallel to the 1 MOhm resistor at the SET pin to ground (as R_{Sense}). The test was carried out by playing a fixed waveform on a mobile phone and transmitting the recorded microphone data by backscattering. The waveform file as well as the received signal were processed and are presented in Fig.9 along with the frequency content for each of these signals in the audible range. We also played a continuous sweep of signals between 100 Hz and 5 kHz, white noise, speech and music signals to test the transmission. The processed backscatter signal's spectrum had some aliasing and a constant sound at 800 Hz, but the audio is still legible . These are artifacts created by our $R_{Baseline}$ and can be rectified by design improvements to the sensor interface and/or signal processing.

4.5 Device Functional Summary

A summary of the power consumption, range and lifetime of the RFSP paired with each of these sensors are provided in Table.1. The table provides sensor specs, RFSP power consumption, measured range with continuous operation at a TX power of 23 dBm and the calculated lifetime for the RFSP when it is augmented with the thin film battery rated 3.9 V and 1 mAh. It is evident that the low-power consumption of the RFSP allows it to function at increased range and can be configured to operate continuously off a thin-film battery for at least one day.

5 RELATED WORK

5.1 RFID and Passive Digital Devices

With the availability of low-power computation modules like the MSP430 and STM ARM cortex processors and ability to produce application specific ICs, small devices that can sense compute and transmit data have been developed. Examples of such devices are the EMG telemetry device described in [20] and the early work on accelerometers powered by RF energy harvesting on WISP [16]. These devices have A/D converters that digitize the sensed signals and a state machine to either perform computation or communicate the data out as packets. They perform these tasks at an impressive power budget as low as 1 mW to 2 mW. With the ability to store

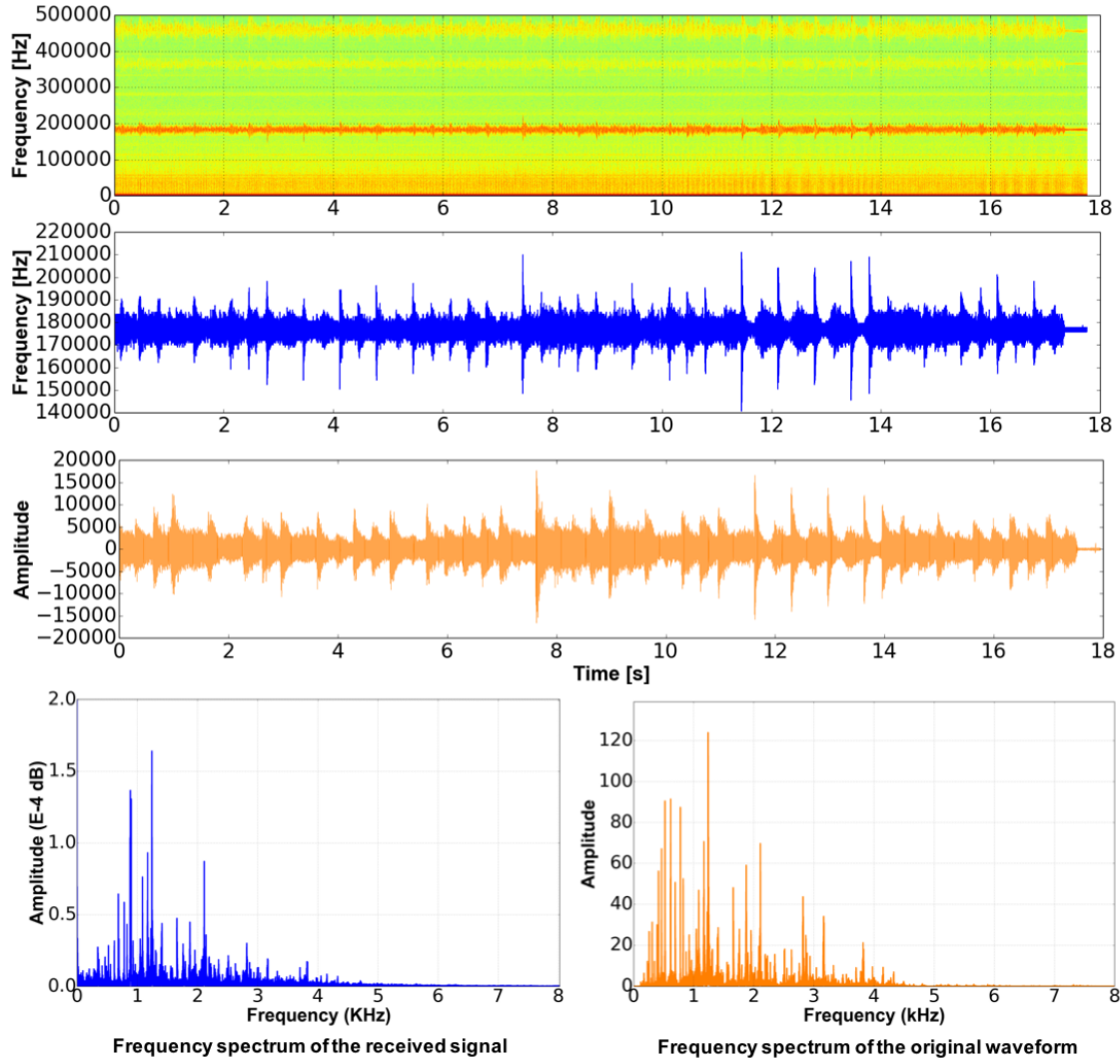


Fig. 7. Received and processed signals for audio signal transmission showing the spectrogram, extracted frequency modulation envelop representing the received waveform (blue), the original waveform played (orange) and the frequency spectrum of the backscattered (blue) and original waveforms (orange) from top to bottom, respectively. Similar to 3 the spectrogram is centered at 915 MHz (0 corresponds to the received 915 MHz carrier). The extracted audio waveform which corresponds with the original waveform. There is some attenuation and distortion in the frequency content when compared to the actual waveform.

harvested energy in supercapacitors and batteries, tasks that require up to several 10's of mW can be handled by these devices only restricted to duty-cycling based on power availability (about 25% duty-cycling for the WISP [16][13]). While these devices come with superior capabilities in terms of sensing and communication, they have more components, consume more power and cost more than a simple design like that of the Great Seal Bug. In this work we try to address the design space between such extremely simple analog sensing device and the more

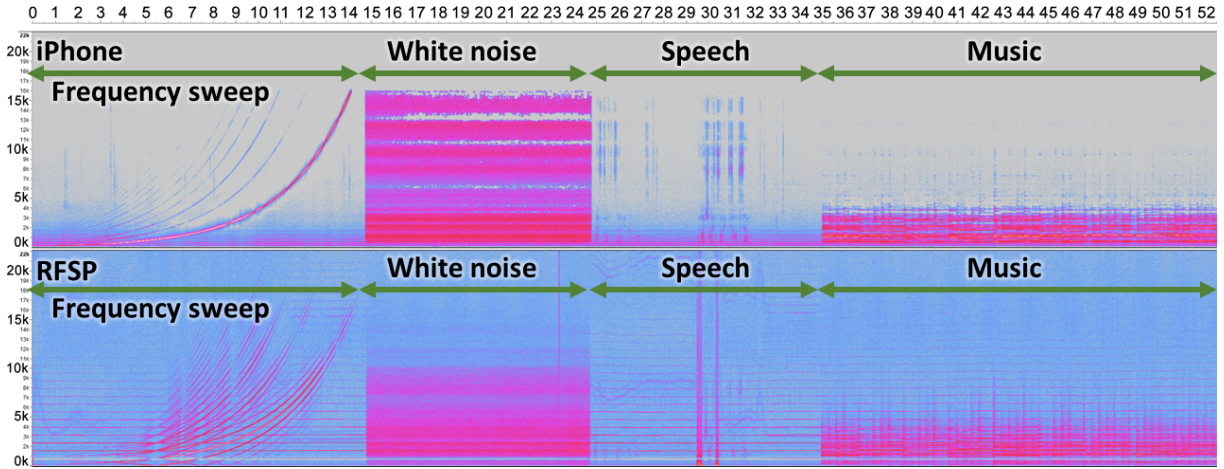


Fig. 8. Spectrogram plots for a continuous frequency sweep, white noise, speech and music audio signal transmission. Top plot is spectrogram of audio signal recorded with an iPhone and the bottom is the spectrogram of signals from the RFSP. The aliasing and a constant noise at 800 Hz is prominent in the bottom figure.

complex digital device. At the same time we demonstrate continuous operation without duty-cycling over a larger physical range with our small power budget ($160 \mu\text{W}$ maximum).

5.2 Hybrid Analog Devices

One of the prior works that addresses the challenge with power and the processing needs proposes a hybrid solution that switches between pure analog operation and digital operation [17]. This work combines the use of a microphone sensor (similar to the Great Seal Bug) with an RFID activation sequence on a WISP. Their analytical model predicts an operational range of 14 ft with the TX power set to 26.7 dBm. In this work we demonstrate the ability of our system to work at this predicted range with lower TX power levels and we also experimentally verify and demonstrate methods to extend the range. Recent work on hybrid devices has led to the development of a battery-free phone, which uses the hybrid technology to establish a connection through using the RFID based digital communication. Once connected it transmits the sound profile through analog backscatter [18]. This system has also demonstrated low-power operation up to 31 ft with duty-cycling based on power availability. One of the methods to harvest more power suggested here is to harvest from multiple bands of frequencies. However, the conclusion that available power was still insufficient for continuous operation of the existing digital processing supports the need to develop analog systems.

5.3 Design Improvements

While the RFSP harvests energy from the 915 MHz continuous wave source, this can also be scaled to other frequencies in the ISM band. The ability to harvest energy from ambient signals like radio, TV and cellular towers and Wi-Fi routers has been demonstrated and their magnitudes are comparable to our power budget [15] [21], [19]. Designing our prototype to harvest energy from different bands would enable powering it using the ambient signals for extended range operation. One of the main challenges with existing single band systems is self-Jamming, where the isolation between the TX and RX is poor and the 915 MHz carrier wave leaks into the receiver module. This becomes a major problem especially when trying to implement the TX and RX on same hardware or close to each other. In either case, the bandwidth and sensitivity for the weak backscattered data is limited due to the presence of the strong carrier signal. One of the solutions proposed for this challenge in

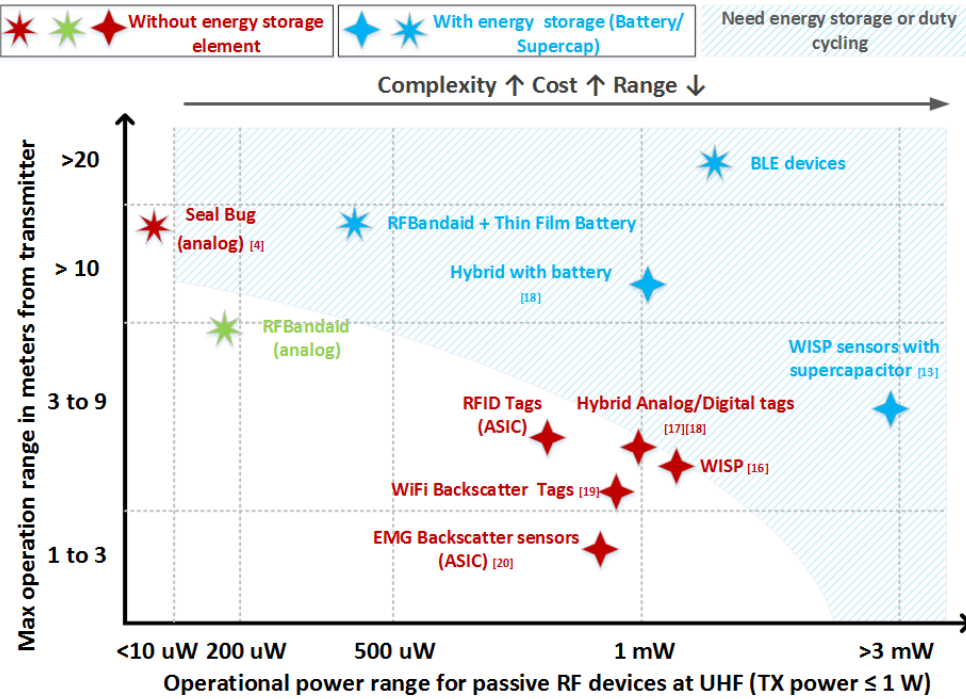


Fig. 9. Representation of the RF devices based on operation scheme (analog/digital), the amount of power consumed and the range between RF tag and receiver for continuous or duty cycles operation. The X axis shows the power consumed and Y axis shows the maximum range capable. The 4 point stars represent Digital devices and the 7 point stars are the analog devices. Color schemes with red indicate battery-free devices and blue are RF devices augmented with energy storage elements. The shaded region in the chart represents the approximate boundary between range that can be supported with continuous operation of a tag while it uses no battery for a given power level in range.

[12] is to use harmonic backscatter, where energy is harvested completely from the 915 MHz while a first or second harmonic is used to backscatter the sensed data. Such devices are designed to use nonlinear components to passively generate a harmonic that can be used for backscatter from device. Another related work uses a tattoo mesh sensor that can be worn on the skin for measuring various parameters [11]. This design implements resistive strain gauge and temperature sensors that are capable of converting the sensed data into frequency modulation. Integrating such a sensor with our low-power device would enable tattoo form-factor sensing using the harvested energy.

5.4 Limitations and Future Work

The RFSP is a minimalistic platform that achieves sensing and communication with a minimum number of components. This enables it to be flexible, small, operate with a low power budget and is easy to use. However, such a minimalistic device comes with some trade-offs and limitations. As seen in Fig. 9, the RF device space has a large number of passive devices that come with digital processing and sensing. However, this addition of an ADC to digitize the sensed signals and a microcontroller to process and transmit them adds an overhead to the power budget of the device. From Fig. 9, this reduces the effective operating range of the device since it requires more power while RF energy available at increasing distances drops as $1/r^2$. On the other end of the spectrum are

fully analog devices (the Great Seal Bug) that transmit the data as amplitude modulations. AM transmission of data have inherently low SNR and noise tolerance. With the RFSP, we have a fully analog platform that harvests energy from a 915MHz continuous wave, senses data, converts it to a frequency modulation and backscatters this as FSK to a remote receiver (RPU). While the RFSP achieves very low power operation (around $160 \mu\text{W}$ max), it comes with some limitations which are listed below along with some solutions for future directions.

- The RFSP does not have any processor on it, hence it does not currently have the ability to process the sensed signal or use any specific protocol to communicate them. It is designed for continuous backscattering of the sensed signals. Microcontrollers can be added to it, although this comes with its own power overhead.
- One of the main limitations here is security of the backscattered data, especially in the medical domain. The data is encoded as FSK and can be easily picked up by a sensitive receiver even 10 meters away. While this work does not focus on adding security features, one of the suggestions for future exploration is to use a low-power XOR logic that adds a pseudo random code to the data and provides a minimum level of security. Another way is to reduce the TX power further (currently tested at 26dBm max) for applications where a large range is not necessary (example, bedside sensing). At a given transmit power level, the RFSP will still have larger operation range than other more complex RFID devices.
- Another limitation with the analog systems lies in the number of such devices that can be deployed simultaneously. While several tens to hundreds of the RFID tags can be used in the same environment, since they use time division multiplexing (TDM) or duty cycling, only a few of the analog sensors can be used with one receiver. Based on the application some of the following methods can be used to avoid collisions when using multiple RFSPs: a) If adding power overhead is permissible, a low-power state machine can be used to enable TDM and anti-collision protocols to the device. b) Another solution that is feasible when different sensors are used with the RFSP in an environment is to divide the bandwidth (10 kHz to 1 MHz) of the RFSP's oscillator to allocate sub-bands (channels) to each RFSP based on the sensor type and application. This also allows simultaneous transmission where different sensor RFSPs identify with a different channel. Moreover, it does not add any power overhead. c) In other applications where the sensors are localized, directional antenna on the RPU can be used to receive data from a specific sensor.
- The RFSP currently has a standard half wave dipole antenna. While this antenna is practical and simple to implement, application specific high-gain antenna design can increase its performance. One of the future directions is to design an inverted-F antenna for on-body applications.

The key features of the RFSP, which include simplicity, modularity, low power consumption and increased range are enablers for new analog sensor and sensing application development. The RFSP's flexibility across multiple sensing domains has been demonstrated in this paper with different types of sensing applications. We have provided results for sensing physiological signals (heart rate, temperature and breathing) as well as for sensing signals with interesting frequency content (audio signals using a microphone). The RFSP is currently designed as a development platform for researchers to explore new sensing methods and solutions for encrypting analog signals. The detailed design specifications for the RFSP are provided and adding sensors or other features to it is a straightforward task. Moreover, the RFSP can be augmented with a thin-film battery and this extends its range to higher than 10 meters as shown in the paper. Adding an energy storage element can also be translated to higher power availability. This supports the power overhead that comes with the use of additional low power digital processing.

6 CONCLUSION

We have so far characterized the RF Bandaid system which is a fully-analog wireless interface for resistive sensors. With the goal of bridging the gap between analog and digital backscatter platforms, we have presented the RFSP that can harvest energy from a dumb 915MHz continuous wave transmitter, measure and map sensor data to

frequency modulations and transmit it out to a RPU using backscatter communication. This effectively moves all digitization and processing to a remote smart receiver, thereby reducing the power consumption, cost and size of the device. Owing to its low power consumption ($40 \mu\text{W}$ and $160 \mu\text{W}$), our device has shown continuous performance at a distance of 4 meters from the transmitter with a transmitted power of 26 dBm. We have also demonstrated the application scenario of deploying this system in a home, by testing sensor data transmission through walls to an RPU placed in a different room at a distance of 9 meters. We envision a bandaid sensor that can be used to sense physiological parameters like heart rate from a patient in a bed. With a transmitter on the bed powering the device, the RPU can be incorporated into a bedside clock that receives, processes and displays sensed data.

We also demonstrated extending the range of the device from the RX up to 9 meters when the device is powered by a small battery. The $160 \mu\text{m}$ thick battery from STMicroelectronics is rated for 1 mAh at 3.9 V and can sustain the device for several hours on a single charge. Finally, to demonstrate the device's ability to measure data from a wide range of sensors (medical and commercial) we have presented measurements for heart rate, breathing rate, temperature and audio data. This prototype was developed on a printed circuit board with COTS devices and was not optimized for space. The device can be shrunk down to a band aid form-factor with a small circuit board on fabric. Adapting better high-gain antenna designs would also optimize the power and data transfer.

REFERENCES

- [1] 2018. Bioharness 3 Activity Monitor. (2018). Retrieved April 18, 2018 from <http://vandrico.com/wearables/device/bioharness-3>
- [2] 2018. Smart Fabrics: The Next Generation in Pressure Mapping. (2018). Retrieved April 18, 2018 from <http://www.boditrak.com/products/smartfabric.php>
- [3] 2018. Spire breath and activity tracker. (2018). Retrieved April 18, 2018 from <https://spire.io/pages/science>
- [4] 2018. The Thing (listening device). (2018). Retrieved April 18, 2018 from [https://en.wikipedia.org/wiki/The_Thing_\(listening_device\)](https://en.wikipedia.org/wiki/The_Thing_(listening_device))
- [5] Datasheet. ADG902 Reflective Switch. (Datasheet). http://www.analog.com/media/en/technical-documentation/data-sheets/ADG901_902.pdf
- [6] Datasheet. BQ25570 Nano Power Boost Charger and Buck Converter for Energy Harvester Powered Applications. (Datasheet). <http://www.ti.com/lit/ds/symlink/bq25570.pdf>
- [7] Datasheet. BUSRPN210 Networked Series. (Datasheet). https://www.ettus.com/content/files/07495_Ettus_N200-210_DS_Flyer_HR_1.pdf
- [8] Datasheet. EnFilm - rechargeable solid state lithium thin film battery. (Datasheet). <http://www.st.com/content/ccc/resource/technical/document/datasheet/group3/4b/31/97/8e/e9/cb/45/4c/DM00408165/files/DM00408165.pdf/jcr:content/translations/en.DM00408165.pdf>
- [9] Datasheet. LTC6906 Micropower Precision Programmable Oscillator. (Datasheet). <http://cds.linear.com/docs/en/datasheet/6906fc.pdf>
- [10] Michael Buettner, Ben Greenstein, Alanson Sample, Joshua R. Smith, and David Wetherall. 2008. Revisiting Smart Dust with RFID Sensor Networks. In *Proc. 7th ACM Workshop on Hot Topics in Networks (Hotnets-VII)*.
- [11] Hohyun Keum, Martin McCormick, Ping Liu, Yong-wei Zhang, and Fiorenzo G Omenetto. 2011. RESEARCH ARTICLES Epidermal Electronics. *Science* 333, September (2011), 838–844. <https://doi.org/10.1126/science.1206157>
- [12] Yunfei Ma, Xiaonan Hui, and Edwin C. Kan. 2016. Harmonic-WISP: A passive broadband harmonic RFID platform. *IEEE MTT-S International Microwave Symposium Digest* 2016–August (2016), 0–3. <https://doi.org/10.1109/MWSYM.2016.7540224>
- [13] S. Naderiparizi, A. N. Parks, Z. Kapetanovic, B. Ransford, and J. R. Smith. 2015. WISPCam: A battery-free RFID camera. *2015 IEEE International Conference on RFID, RFID 2015* (2015), 166–173. <https://doi.org/10.1109/RID.2015.7113088>
- [14] Pavel Nikitin, A.N. Parks, and Joshua R. Smith. 2012. RFID-Vox: A Tribute to Leon Theremin. In *Wirelessly powered sensor networks and computational RFID*, Joshua R. Smith (Ed.). Springer SBM.
- [15] Aaron N. Parks and Joshua R. Smith. 2014. Sifting through the airwaves: Efficient and scalable multiband RF harvesting. *2014 IEEE International Conference on RFID, IEEE RFID 2014* (2014), 74–81. <https://doi.org/10.1109/RID.2014.6810715>
- [16] A.P. Sample, D.J. Yeager, P.S. Powledge, A.V. Mamishev, and J.R. Smith. 2008. Design of an RFID-Based Battery-Free Programmable Sensing Platform. *IEEE Transactions on Instrumentation and Measurement* 57, 11 (November 2008), 2608–2615.
- [17] V. Talla, M. Buettner, D. Wetherall, and J. Smith. 2013. Hybrid Analog-Digital Backscatter Platform for High Data Rate, Battery-Free Sensing. In *Wireless Sensors and Sensor Networks (WiSNet), 2013 IEEE Topical Conference on*.
- [18] Vamsi Talla, Bryce Kellogg, Shyamnath Gollakota, and Joshua R. Smith. 2017. Battery-Free Cellphone. *Proceedings of the ACM on Interactive, Mobile, Wearable and Ubiquitous Technologies* 1, 2 (2017), 1–20. <https://doi.org/10.1145/3090090>

- [19] Vamsi Talla, Bryce Kellogg, Benjamin Ransford, Saman Naderiparizi, Shyamnath Gollakota, and Joshua R. Smith. 2015. Powering the Next Billion Devices with Wi-Fi. (2015). <https://doi.org/10.1145/1235> arXiv:1505.06815
- [20] Stan J Thomas, Reid R Harrison, Anthony Leonardo, and Matthew S Reynolds. 2012. A battery-free multichannel digital neural/EMG telemetry system for flying insects. *Biomedical Circuits and Systems, IEEE Transactions on* 6, 5 (2012), 424–436.
- [21] Hubregt J. Visser, A. C F Reniers, and J. A C Theeuwes. 2008. Ambient RF energy scavenging: GSM and WLAN power density measurements. *Proceedings of the 38th European Microwave Conference, EuMC 2008 October* (2008), 721–724. <https://doi.org/10.1109/EUMC.2008.4751554>

7 APPENDIX

